Bollettino di Geofisica Teorica ed Applicata Vol. 53, n. X, pp. x-xx; Xxxxxxx 2012
DOI 10.4430/bgta0064

The 2002 Mount Sernio and the 2004 Kobarid sequences: static stress changes and seismic moment release

C. Barnaba and G. Bressan

Istituto Nazionale di Oceanografia e di Geofisica Sperimentale, Cussignacco (Udine), Italy

(Received: January 26, 2012; accepted: May 29, 2012)

ABSTRACT We analyze the aftershock sequences caused by the 2002 M_D 4.9 and the 2004 M_D 5.1 mainshocks, occurred in the Friuli area and western Slovenia, with two different approaches. The Coulomb stress changes induced by the mainshocks were calculated to explore the interaction with the aftershock patterns. The aftershock decay is investigated analyzing the temporal behaviour of cumulative seismic moment released, derived from a static fatigue model. The Coulomb stress changes, calculated on the receiver fault of the largest aftershock, show that the aftershock sequences are mostly located in a stress shadow zone. The modelling of Coulomb stress variations, that incorporates the regional stress field, fits better the aftershock pattern. The lack of correlation between the Coulomb stress perturbations and part of the aftershocks is attributed to stress heterogeneities not accounted in the model. The decay rate of the seimic moment release is different in the 2002 and 2004 sequences. According to this model, the distribution of stress in the aftershock volume appears more uniform in the 2004 sequence. Stress fluctuations induced by the mechanical heterogeneities of the medium is suggested by the static fatigue modelling, particularly for the 2002 sequence.

Key words: Coulomb stress changes, static fatigue, aftershocks, Friuli, Slovenia.

1. Introduction

The aftershocks of an earthquake are commonly interpreted as a process of relaxing stress concentration caused by the rupture of the mainshock. The understanding of the mechanism of aftershock sequences has been the goal of several investigations because of its strong implications for earthquake nucleation and the physical properties of a fault zone. Dieterich (1994) derived a model where the aftershock nucleations are promoted by a shear stress step induced by the dynamics of the mainshock, with the rate of earthquake occurrence related to the stressing rate. In this model, the aftershock occurrence depends on the amplitude of the stress jump, the rate and slip dependence of friction strength and the effective normal stress of the faults, and the background seismicity rate. The modelling of the Coulomb stress changes induced by a mainshock has been widely used in recent years to investigate the stress transfer and earthquake triggering. Several studies have pointed out the correlation between the pattern of aftershocks and the zone of increased Coulomb stress changes (King *et al.*, 1994; Nostro *et al.*, 1997; Miller *et al.*, 2004, and many others). In particular, Lin and Stein (2004) explored the main aspects of Coulomb stress transfer associated with thrust events. A

recent development of the method was performed by Toda *et al.* (2005), who calculated successive stress changes associated with multiple mainshocks, coupling the static stress changes to rate and state friction model of Dieterich (1994). Scholz (1990) considered aftershocks to be a secondary process induced by the dynamic rupture effect of the mainshock. Scholz (1990) interpreted the aftershocks as a delayed fracturing process caused by static fatigue. The static fatigue implies a time-dependent weakening following the mainshock stress change. Aftershocks occur on asperities that experience high stress induced by the mainshock and gradual weakening until they fail.

In this paper, we calculate the Coulomb stress perturbations caused by the 2002 M_D 4.9 Mount Sernio mainshock and the 2004 M_D 5.1 Kobarid mainshock to examine the relation with the aftershock patterns. M_D is the coda-duration magnitude, calculated according to Rebez and Renner (1991). Furthermore, the cumulative seismic moment released in the aftershock sequences is analyzed with the model of Marcellini (1995a), based on a static fatigue approach.

2. The seismic sequences

The 2002 Mount Sernio sequence (Fig. 1) is relocated with the tomographic velocity model of Gentile *et al.* (2000). The sequence occurred in the central part of the Friuli area (north-eastern Italy), starting on February 14 with the M_D 4.9 mainshock and lasted till the end of May (Gentili and Bressan, 2008). The tectonic pattern of the area is mainly characterized by E-W trending thrusts and backthrusts, displaced by minor vertical faults NNW-SSE and NNE-SSW oriented. The mainshock is located at 13.5 km depth. The aftershocks retained after the magnitude cut-off for catalogue completeness (M_D 1.5) are about 30, located between 3 and 15 km depth. The *p*-value of the Omori's regression is 0.80 (Gentili and Bressan, 2008). The mainshock is characterized by a focal mechanism of prevailing thrusting with small strike-slip component. It is related to a thrust striking about E-W and dipping about 40° to the north. The focal mechanism of the largest aftershock (M_D 3.2) shows thrust motion that is attributed to a minor reverse fault, WNW-ESE oriented and dipping 60° to NNE.

The 2004 Kobarid sequence (Fig. 2) started on July 12 with a mainshock of M_D 5.1. The sequence occurred in western Slovenia, near the Italian border and is relocated with the tomographic velocity model of Bressan *et al.* (2009). The earthquakes are located along the Ravne fault (Kastelic *et al.*, 2008), a near vertical dextral strike-slip fault, about NW-SE oriented. The pattern of the tomographic images of Bressan *et al.* (2009) suggests that the Ravne fault zone is characterized by branching and bending. The number of aftershocks retained for the completeness of the catalogue (M_D 2.0) is 166, in a time window of 138 days, till the end of November 2004 (Gentili and Bressan, 2008). The mainshock is located at about 6 km depth and the aftershocks appear clustered in space and located mainly between 4 and 6 km depth. The temporal decay of the aftershocks is expressed by *p*-value 1.04 of the Omori's regression (Gentili and Bressan, 2008). The fault plane solutions of the mainshock and of the largest aftershock (M_D 3.6) show strike-slip mechanism related to dextral strike-slip motion along the Ravne fault (Bressan *et al.*, 2009).

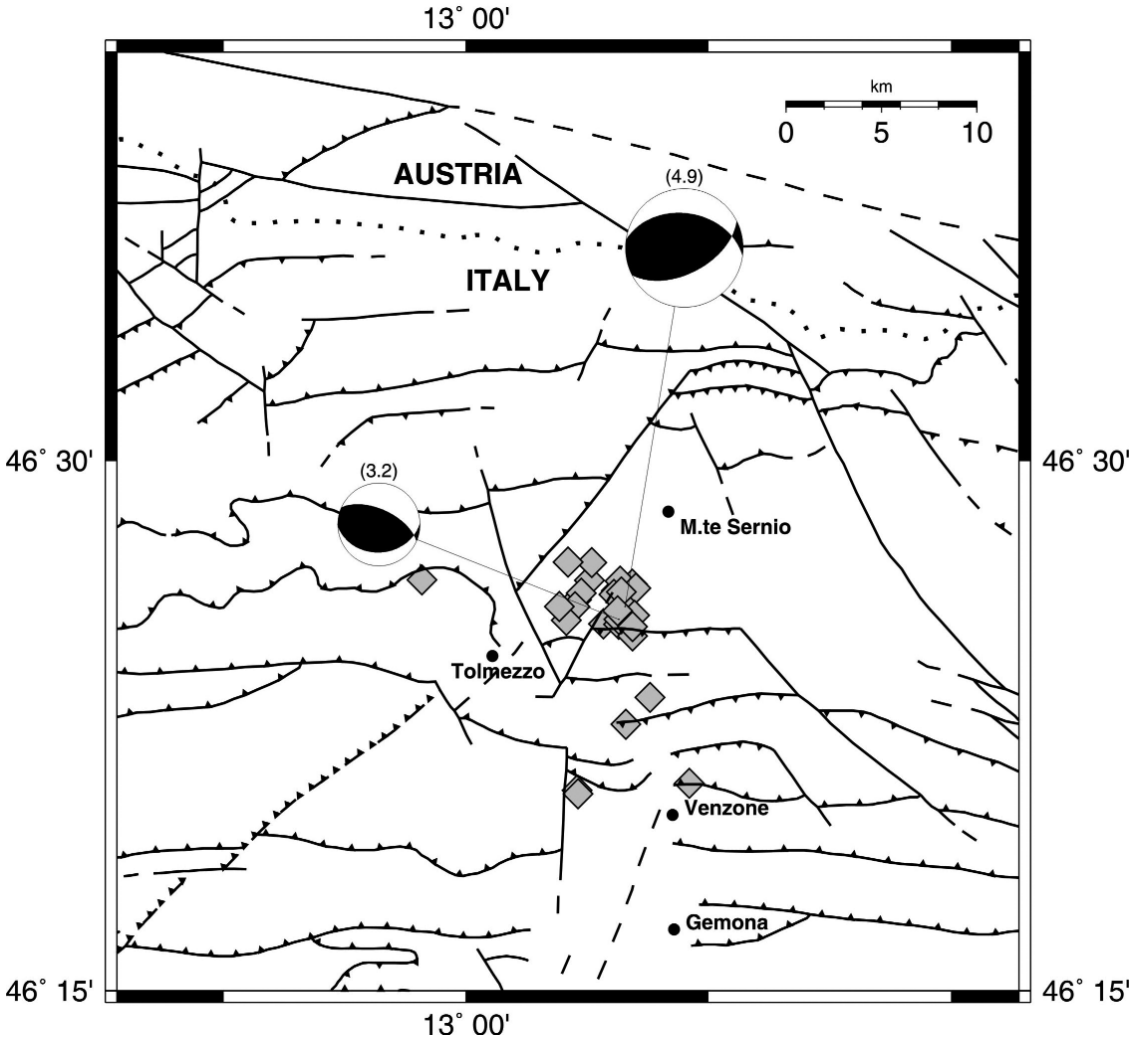

Fig. 1 - Map of the 2002 Mount Sernio sequence (diamonds), with the focal mechanisms of the mainshock (larger size) and of the largest aftershock. The coda-duration magnitude is shown in parentheses. Solid and dashed lines: subvertical faults, barbed lines: thrust. Dots mark national boundaries. The main toponyms are also shown.

3. Static stress changes

The static stress changes are calculated using Okada's (1992) equations for dislocations on rectangular planes embedded in a homogeneous and isotropic half-space (King *et al.*, 1994; Stein *et al.*, 1994).

The static stress changes are expressed as changes in the Coulomb failure function ΔCFF, defined as:

$$\Delta CFF = \Delta\tau + \mu(\Delta\sigma_n + \Delta P) \quad (1)$$

where $\Delta\tau$ is the shear stress change in the direction of fault slip, μ is the friction coefficient, $\Delta\sigma_n$

is the change in normal stress (positive for extension) and ΔP is the change in pore pressure.

The change ΔP in pore pressure is given, under undrained conditions, as:

$$\Delta P = -B\frac{\Delta\sigma_{kk}}{3} \tag{2}$$

where B is the Skempton's coefficient of the rock-fluid mixture and $\Delta\sigma_{kk}$ is the volumetric stress change. The Skempton's coefficient theoretically ranges from 0 to 1, depending on the level of fluid saturation (Roeloffs, 1988). The volumetric stress change can be approximated as $\frac{\Delta\sigma_{kk}}{3} \cong \Delta\sigma_n$, assuming that fault zone materials (Rice, 1992; Harris, 1998) are more ductile than the surrounding rocks. Therefore Eq. (1) may be rewritten as:

$$\Delta CFF = \Delta\tau + \mu'(\Delta\sigma_n) \tag{3}$$

where $\mu'=\mu(1-B)$ is the effective coefficient of friction. Positive values of static stress changes encourage failure while negative ones move a fault away from failure.

In the present study we investigate the relation between the aftershock pattern and the static stress changes caused by the 2002 M_D 4.9 Mount Sernio and the 2004 M_D 5.1 Kobarid mainshocks. In both cases, the static stress changes are calculated with Poisson's ratio 0.25, shear modulus $3.2\cdot10^4$ MPa, assuming coefficient of friction 0.8 and Skempton's coefficient 0.47. The fault dimensions are derived from the relationships of Wells and Coppersmith (1994).

Firstly, we analyze the Coulomb stress variations induced by the 2002 February 14 event, which occurred in the Friuli area with M_D 4.9. The 2002 main rupture is approximated by a thrust rectangular fault with dimensions 1.4 km·1.5 km, with strike 278°, dip 42° and rake 118°, as resulting from the focal mechanism. The top and the bottom of the main fault are placed at 13.0 and 14.0 km, respectively. The seismic moment is $1.27\cdot10^{16}$ Nm (Saraò, 2006). Fig. 3 shows the Coulomb stress changes caused by the 2002 mainshock on the thrust plane of the largest aftershock (M_D 3.2), on a horizontal map at 13.5 km depth and on a vertical cross section perpendicular to the fault plane. The receiver fault is striking 294°, dipping 60° with rake 104°. The minor number of aftershocks (about 40%) is located in the area of increased static stress change. Figs. 4 and 5 show the separate contribution of shear and normal stress changes, respectively. Most of the aftershocks fall in the area of decreased shear stress changes (stress shadow zone) while the opposite is true with normal stress changes, where about 60% of the aftershocks occurs in the area of increased normal stress. Furthermore, we include in the calculation of static stress changes the effect of regional stress field, that in this area is characterized by a thrusting regime (Bressan *et al.*, 2003), with maximum principal stress striking 359° and plunging 6°, intermediate principal stress 95° oriented with plunge 44° and minimum principal stress with azimuth 263° and plunge 45°. The magnitude of the regional stress field is assumed to be 15 bars (Perniola *et al.*, 2004). According to King *et al.* (1994), the optimally oriented planes where aftershocks are expected to occur are determined by the total stress tensor given by the co-seismic stress change of the mainshock and by the regional stress. The optimally oriented planes for failure are those where the total stress tensor is maximized.

The pattern of the Coulomb stress changes caused by the 2002 mainshock is slightly altered

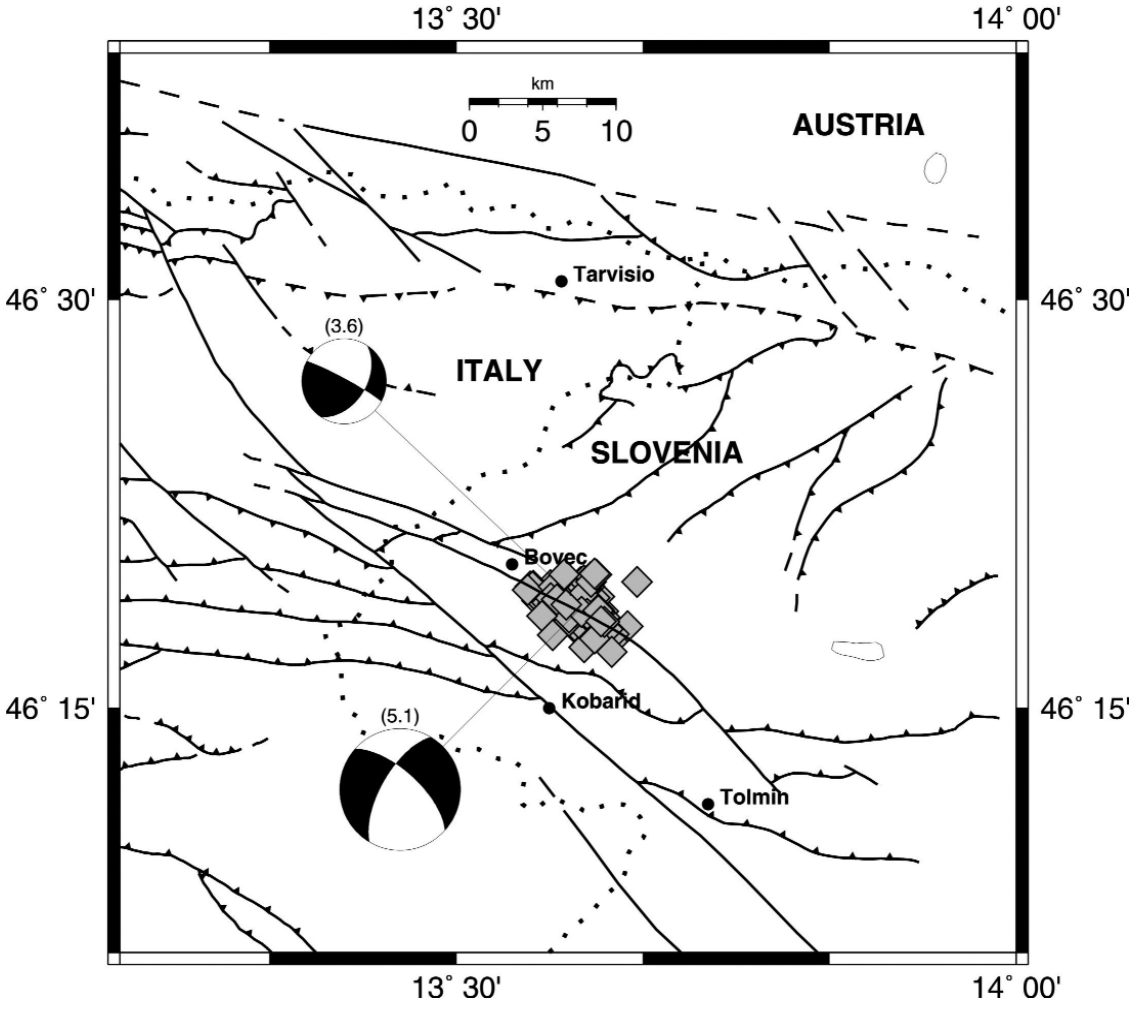

Fig. 2 - Map of the 2004 Kobarid sequence (diamonds), with the focal mechanisms of the mainshock (larger size) and of the largest aftershock. The coda-duration magnitude is shown in parentheses. The main toponyms are also shown. Other symbols as in Fig. 1.

when including the effect of the regional stress field. About 50% of the aftershocks fall in the area of increased static stress change (Fig. 6). The same percentage results when considering the separate contribution of shear stress changes (Fig. 7). The percentage of the aftershocks located in the positive normal stress change region is about 65% (Fig. 8).

The static stress changes generated by the 2004 July 12 event, occurred in the western Slovenia with M_D 5.1, are then modelled. The rupture geometry of the mainshock consists of right-lateral strike-slip rectangular fault, 3.3 km long and 3.2 km wide, with strike 312°, dip 66° and rake -153°, as resulting from focal mechanism. The top and the bottom of the main fault are placed at 3.8 and 7 km, respectively. The seismic moment is $4.5 \cdot 10^{16}$ Nm (Saraò, 2006). The Coulomb stress variations induced by the 2004 mainshock were calculated on the target fault of

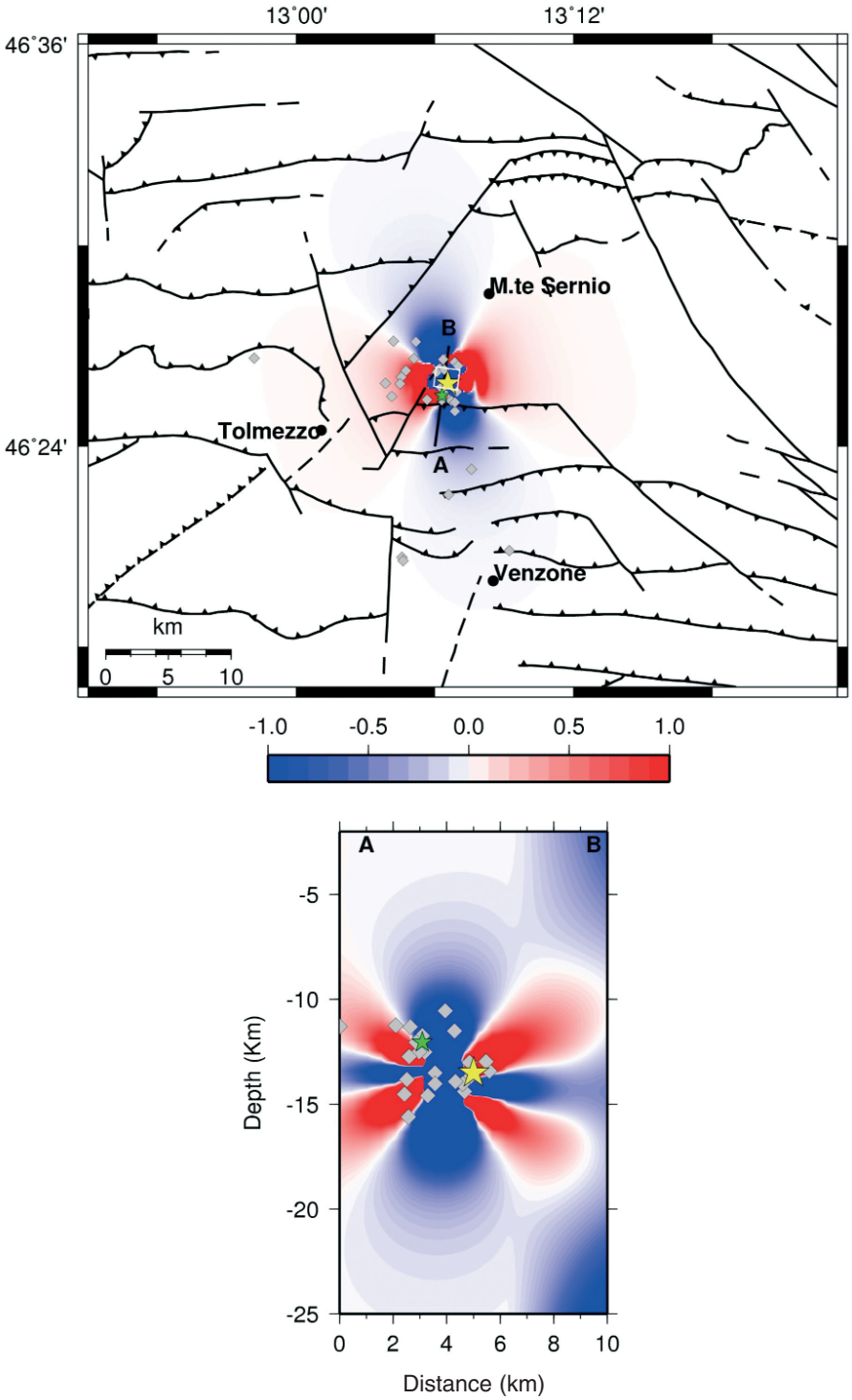

Fig. 3 - Coulomb stress changes (in bar) caused by the 2002 Mount Sernio mainshock (yellow star) resolved on the fault plane of the largest aftershock (green star). Map view at 13.5 km depth and vertical cross section perpendicular to the fault strike of the largest aftershock. The 2002 aftershocks are marked by diamonds. Solid white lines indicate the surface projection of the main shock fault. Other symbols are as in Fig. 1.

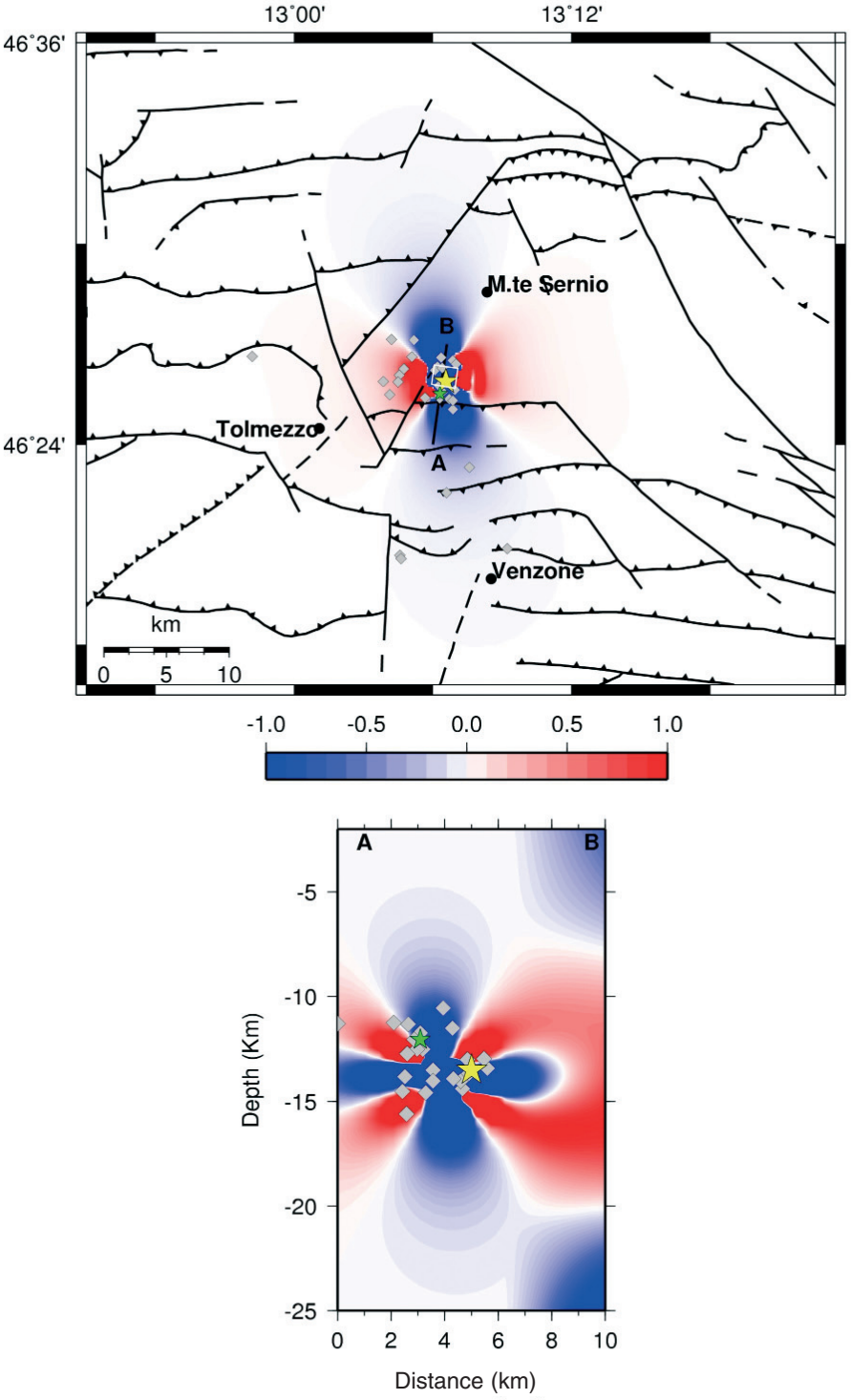

Fig. 4 - Shear stress changes (in bar) caused by the 2002 Mount Sernio mainshock resolved on the fault plane of the largest aftershock. Map orientations and symbols are as in Figs. 1 and 3.

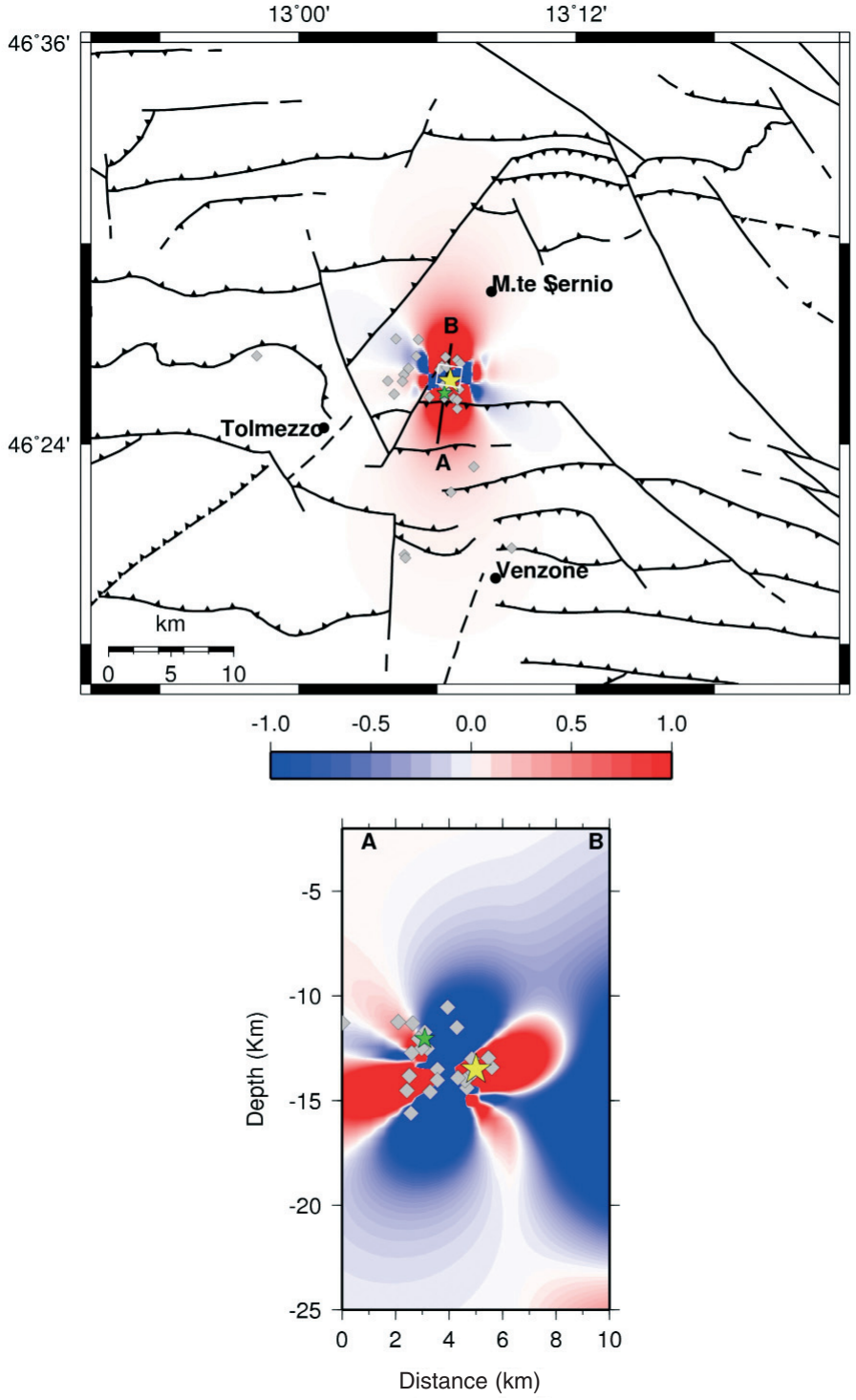

Fig. 5 - Normal stress changes (in bar) caused by the 2002 Mount Sernio mainshock resolved on the fault plane of the largest aftershock. Map orientations and symbols are as in Figs. 1 and 3.

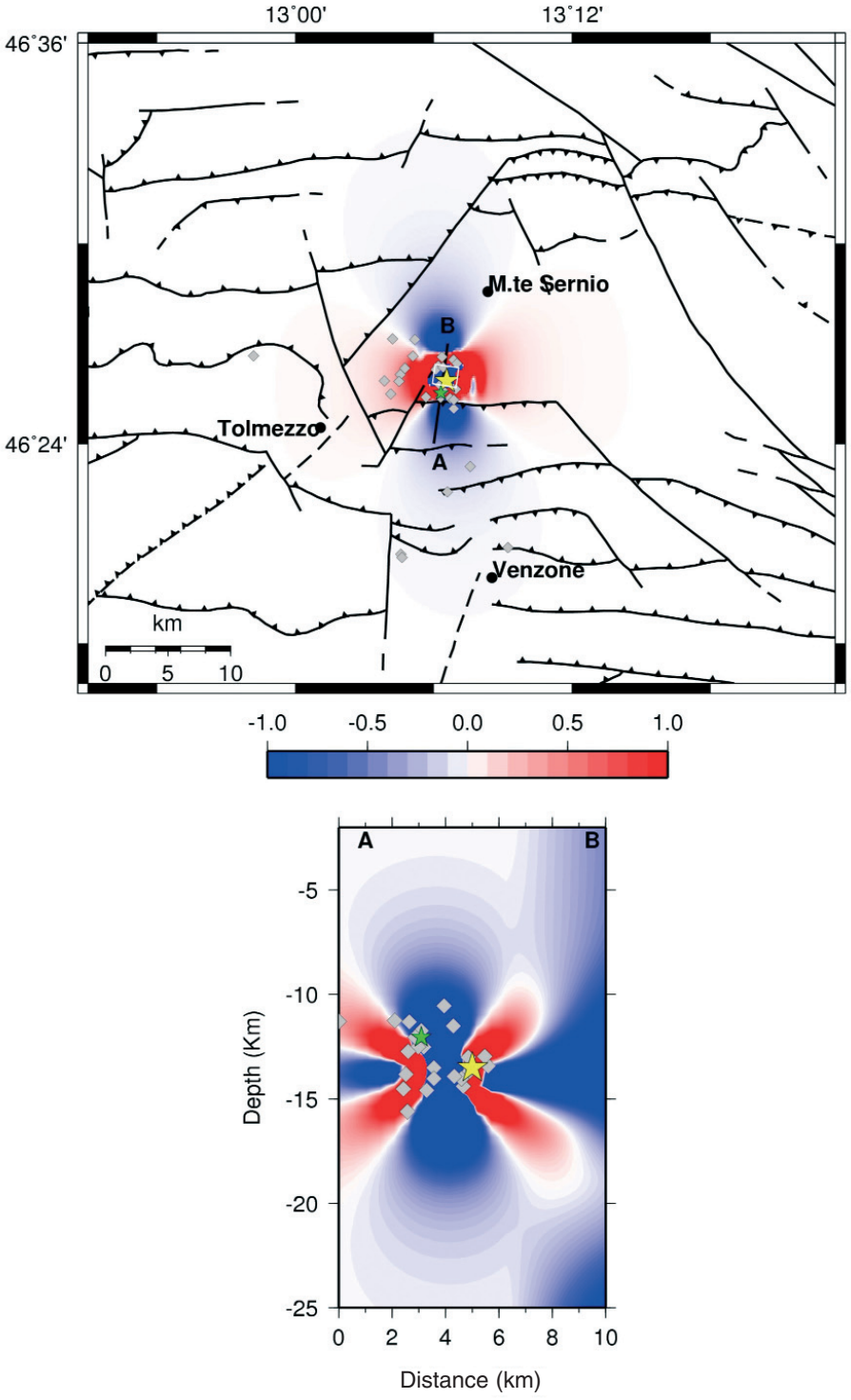

Fig. 6 - Coulomb stress changes (in bar) caused by the 2002 Mount Sernio mainshock, taking into account the regional stress field. Map orientations and symbols are as in Figs. 1 and 3.

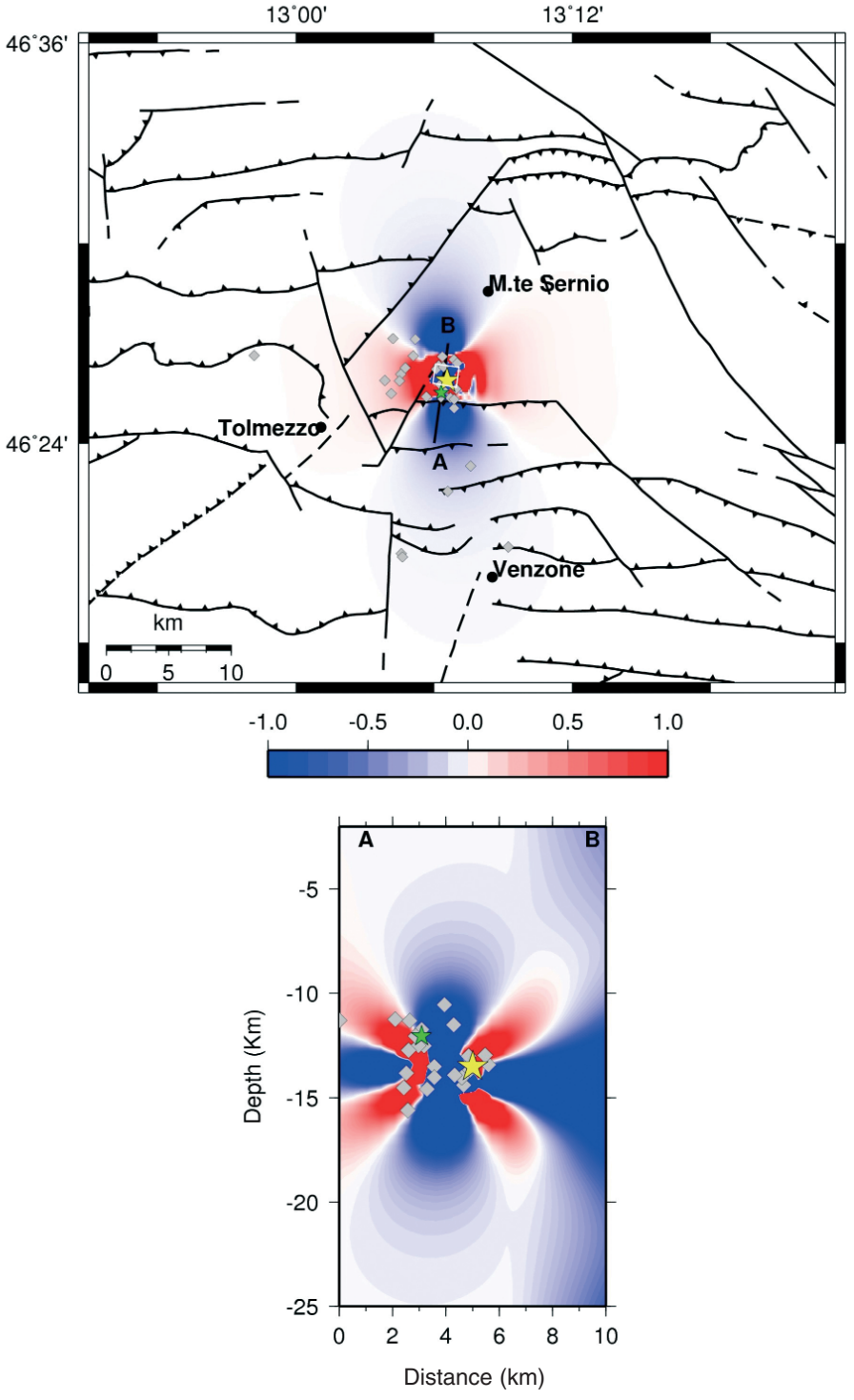

Fig. 7 - Shear stress changes caused (in bar) by the 2002 Mount Sernio mainshock, taking into account the regional stress field. Map orientations and symbols are as in Figs. 1 and 3.

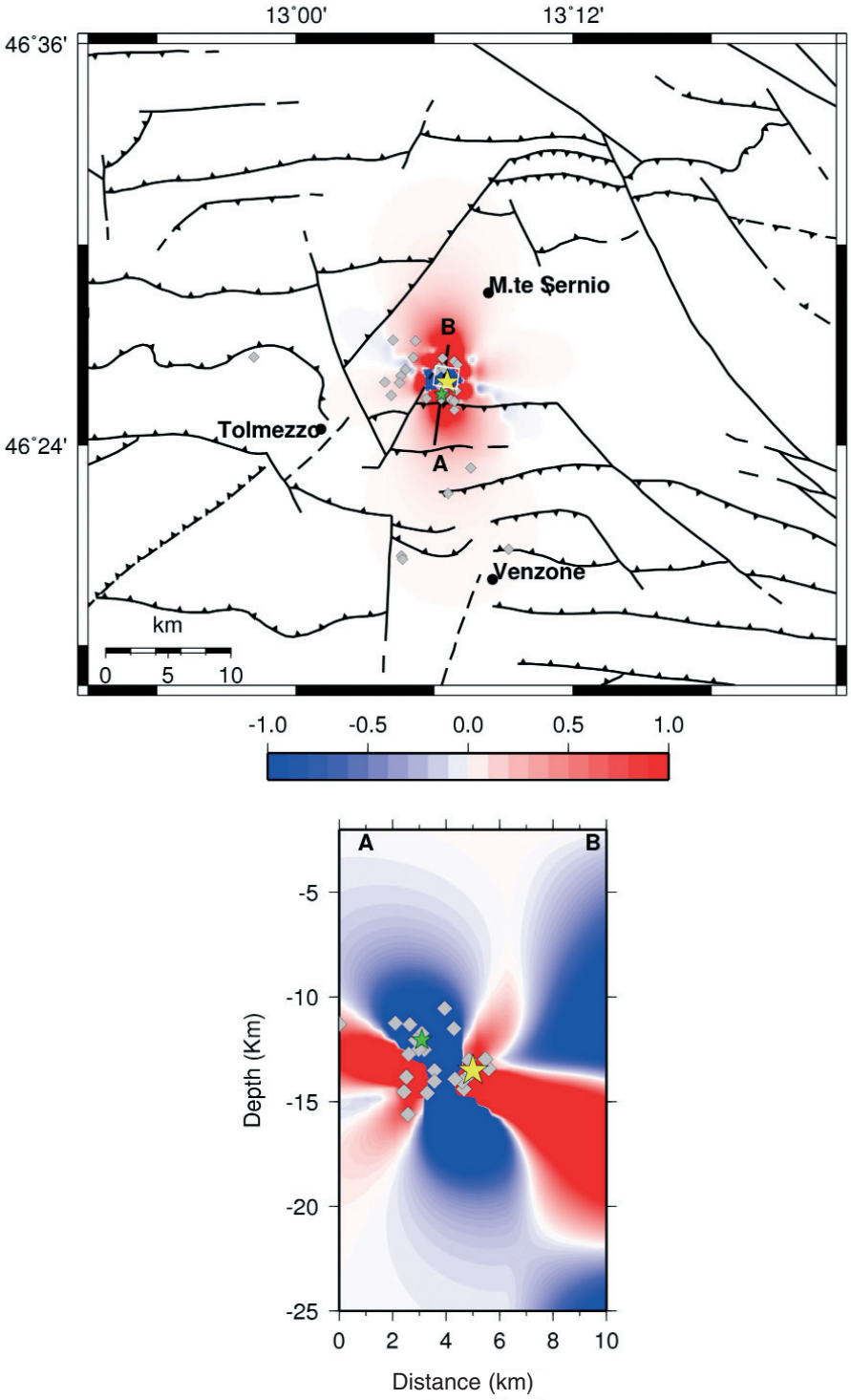

Fig. 8 - Normal stress changes (in bar) caused by the 2002 Mount Sernio mainshock, taking into account the regional stress field. Map orientations and symbols are as in Figs. 1 and. 3.

the largest aftershock (M_D 3.6), striking 298°, with dip 84° and rake 137°. The results are shown on a horizontal map at 5 km depth and on a vertical cross section perpendicular to the fault plane (Fig. 9). The static stress changes decrease in the area where most of the aftershocks are located. The separate contribution of shear and normal stress changes are shown in Figs. 10 and 11, respectively. Most of the aftershocks are located in the area of negative shear stress changes. About 30% of the earthquakes occurs in the area associated to positive normal stress changes. Afterwards, we include the regional stress field in the calculation of the static stress changes. The regional stress field acting in this area (Bressan *et al.*, 2003) is characterized by a strike-slip regime with maximum principal stress striking 351° and plunging 4°, intermediate principal stress 240° oriented with plunge 78° and minimum principal stress with azimuth 82° and plunge 11°. The amplitude of the regional stress field is assumed to be 15 bars (Perniola *et al.*, 2004). Aftershock occurrence tends to concentrate (about 75%) in the areas of increased static stress changes (Fig. 12) and of shear stress changes (Fig. 13). A minor percentage (38%) fall in the positive normal stress changes area (Fig. 14).

4. Aftershock temporal behaviour

The aftershock temporal behaviour is investigated according to the Marcellini's (1995a, 1995b, 1997) model, based on the experimental static fatigue relation of Zhurkov (1965):

$$S(t_i) = d\sigma + \frac{RT}{\gamma} \cdot \ln t_i / t_0 \qquad (4)$$

where $S(t_i)$ is the cumulative stress drop of the sequence events, $d\sigma$ is the dynamic stress step of the mainshock at the origin time t_0, R the universal gas constant, T the absolute temperature, t_i the time after the mainshock of the i-th aftershock and γ a constant, related to the molecular structure disorientation caused by the applied stress (Zhurkov, 1965), t_0 is set 1 arbitrarily.

The model is based on the following stress conditions. When mainshock occurs, the stress in the focal volume is given by the sum of the static stress just before the event and the dynamic stress step caused by the dynamic rupture effect. The dynamic stress step causes a steady increase of the stress intensity factor on unbroken asperities on the main fault plane and on its surroundings. The crack grows quasi-statically up to failure on the asperities, with a time delay depending on the initial value of the stress intensity factor. According to this model, aftershocks are delayed fractures that occur with a time depending on the initial stress applied. Aftershock i occurs at time t_i with stress drop $\Delta\sigma_i$, followed by another aftershock at time $t_i+\Delta t_i$ and so on, until the stress concentration is relaxed. As pointed out by Scholz (1972), rocks and generally brittle materials are characterized by strength which is time dependent. Scholz (1990) interpreted the aftershock sequences as a delayed fracturing process caused by static fatigue. The dynamic step induced by the mainshock may load the neighbouring zones to stresses much higher than their long-term strength. These zones will fail by static fatigue process with delay time depending on the induced stress level.

Taking the relation $M_0=\Delta\sigma V$ (Madariaga, 1979), where M_0 is the seismic moment, $\Delta\sigma$ the stress drop and V the focal volume, Eq. (4) becomes:

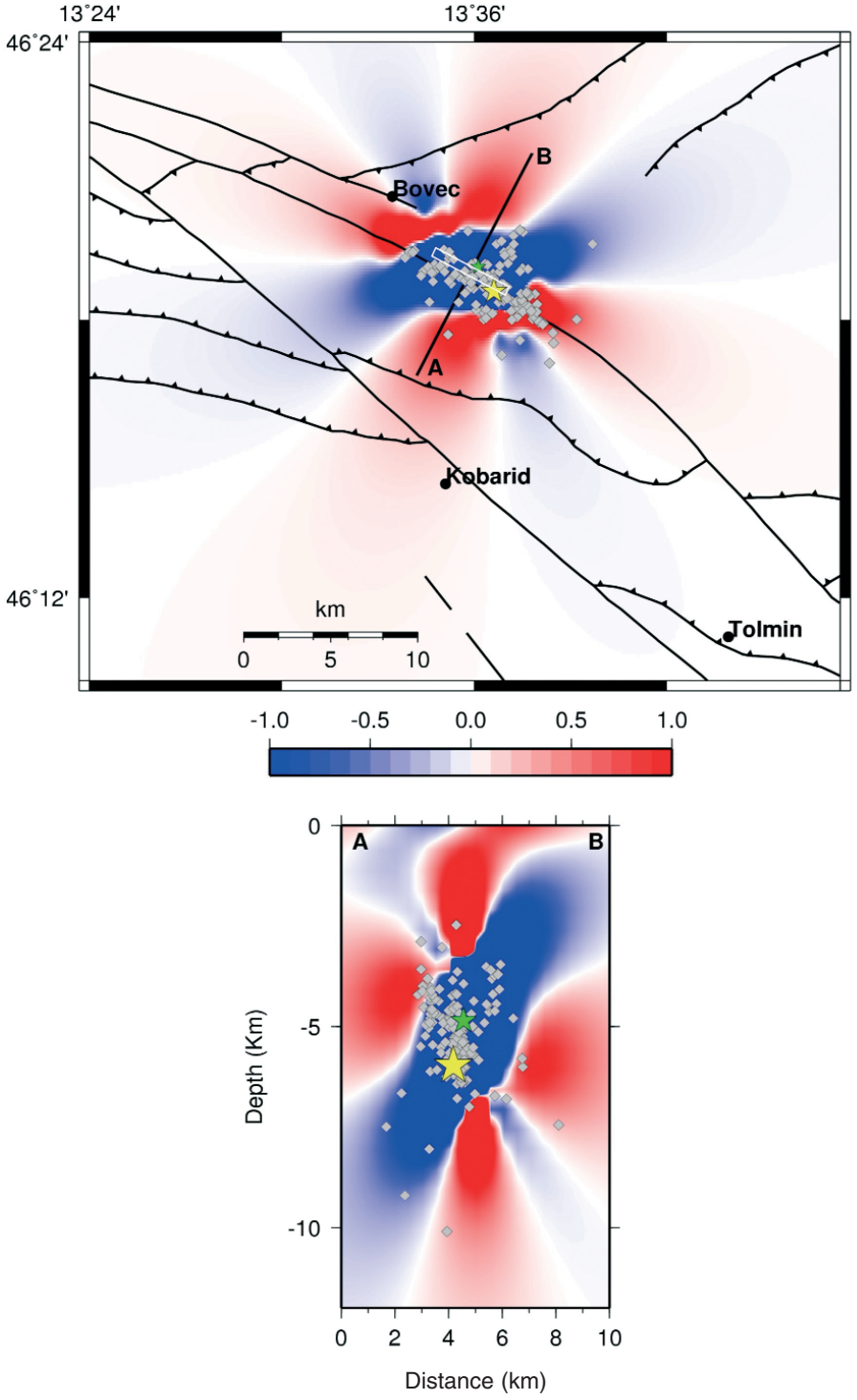

Fig. 9 - Coulomb stress changes (in bar) caused by the 2004 Kobarid mainshock (yellow star) resolved on the fault plane of the largest aftershock (green star). Map view at 5 km depth and vertical cross section perpendicular to the fault strike of the largest aftershock. The 2004 aftershocks are marked by diamonds. Solid white lines indicate the surface projection of the main shock fault. Other symbols are as in Fig. 2.

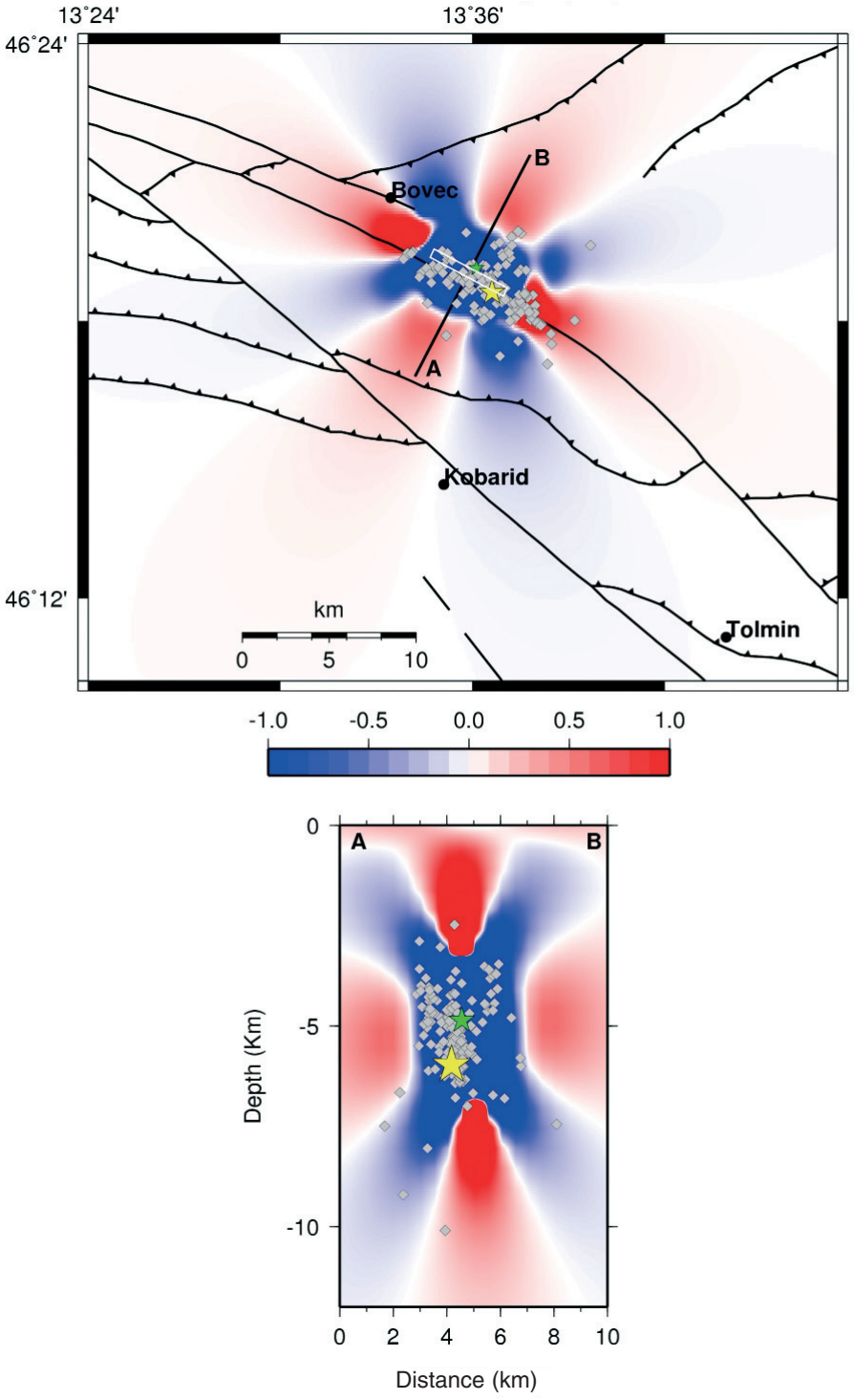

Fig. 10 - Shear stress changes (in bar) caused by the 2004 Kobarid mainshock resolved on the fault plane of the largest aftershock. Map orientations and symbols are as in Figs. 9 and 2.

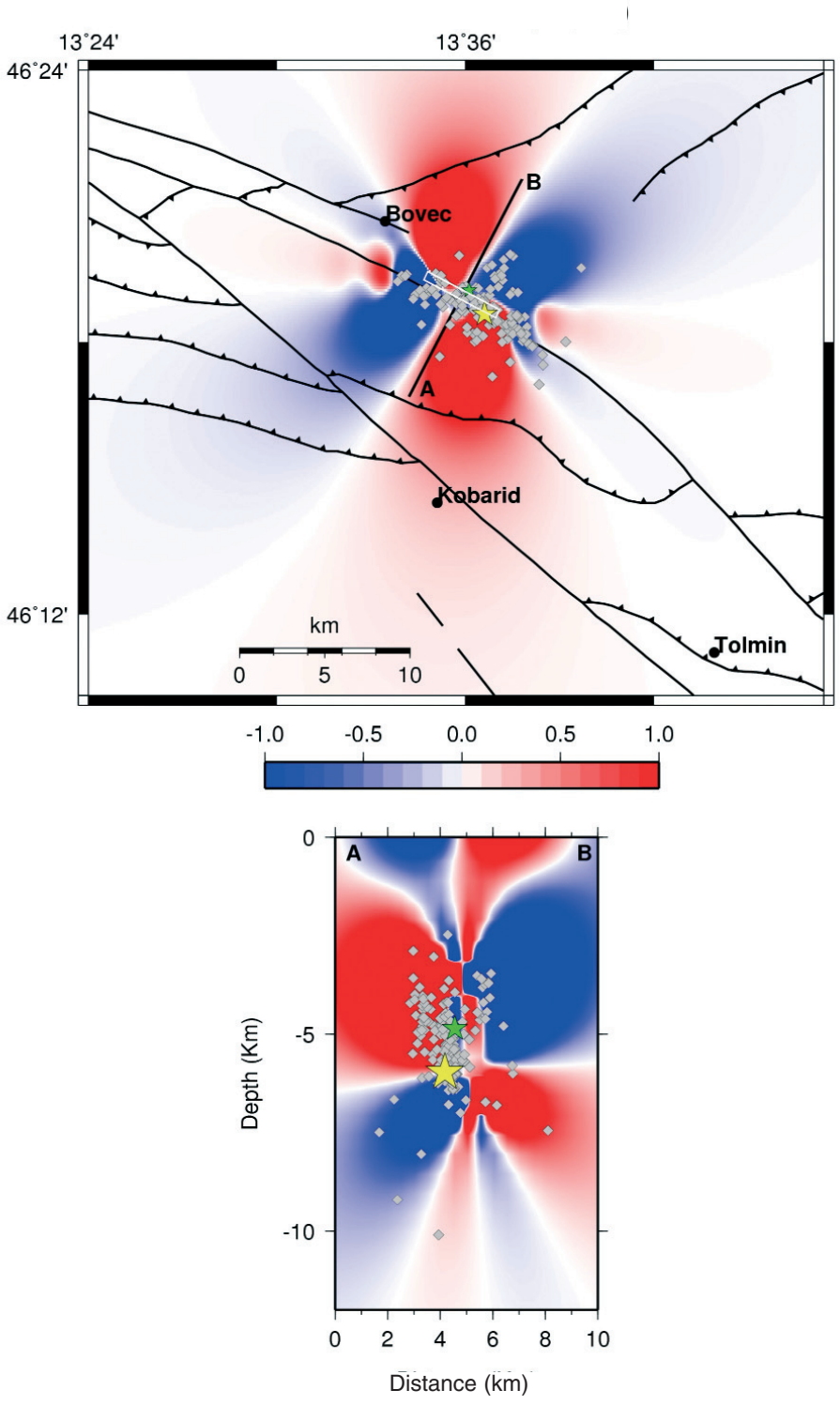

Fig. 11 - Normal stress changes (in bar) caused by the 2004 Kobarid mainshock resolved on the fault plane of the largest aftershock. Map orientations and symbols are as in Figs. 9 and 2.

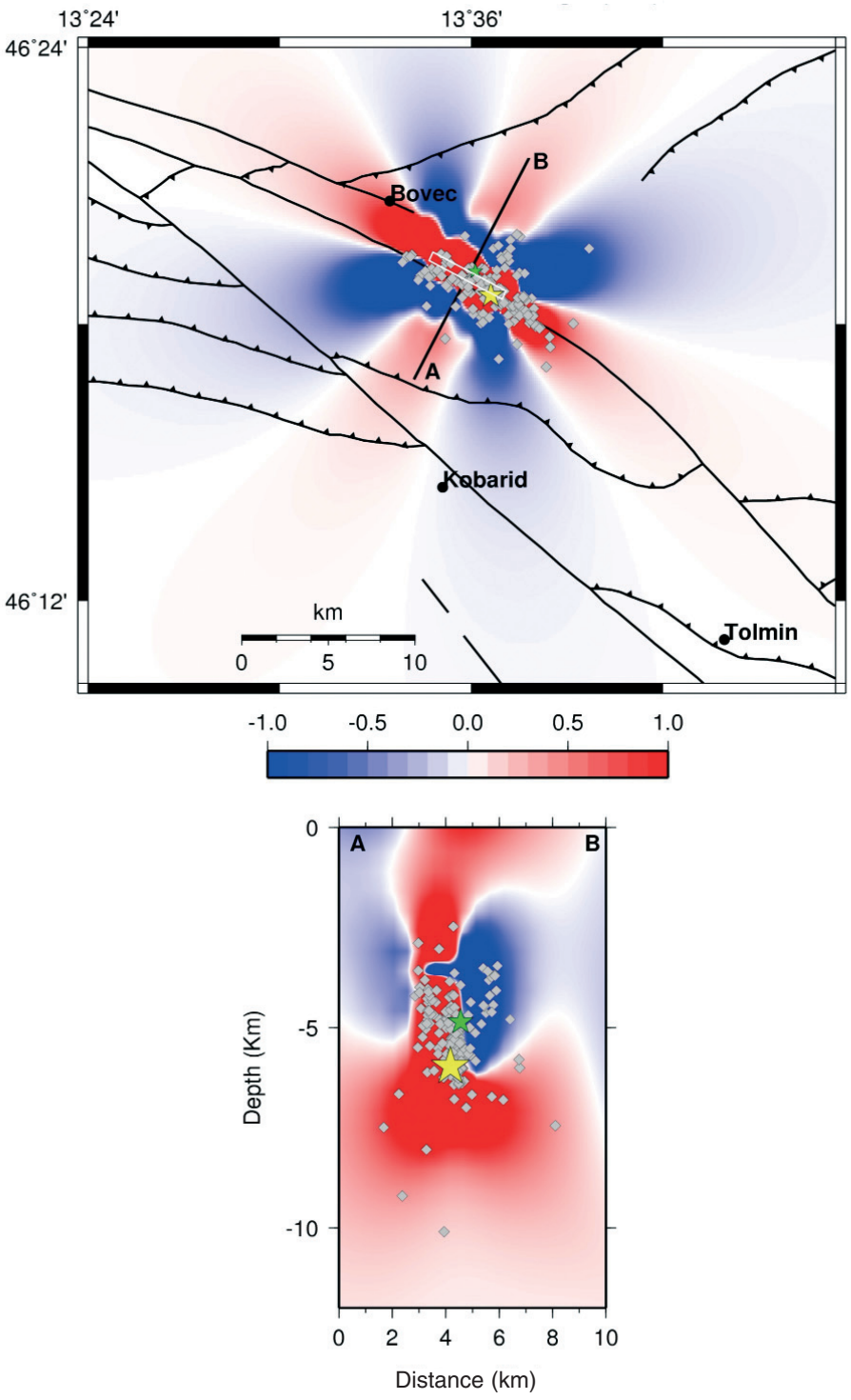

Fig. 12 - Coulomb stress changes (in bar) caused by the 2004 Kobarid mainshock, taking into account the regional stress field. Map orientations and symbols are as in Figs. 9 and 2.

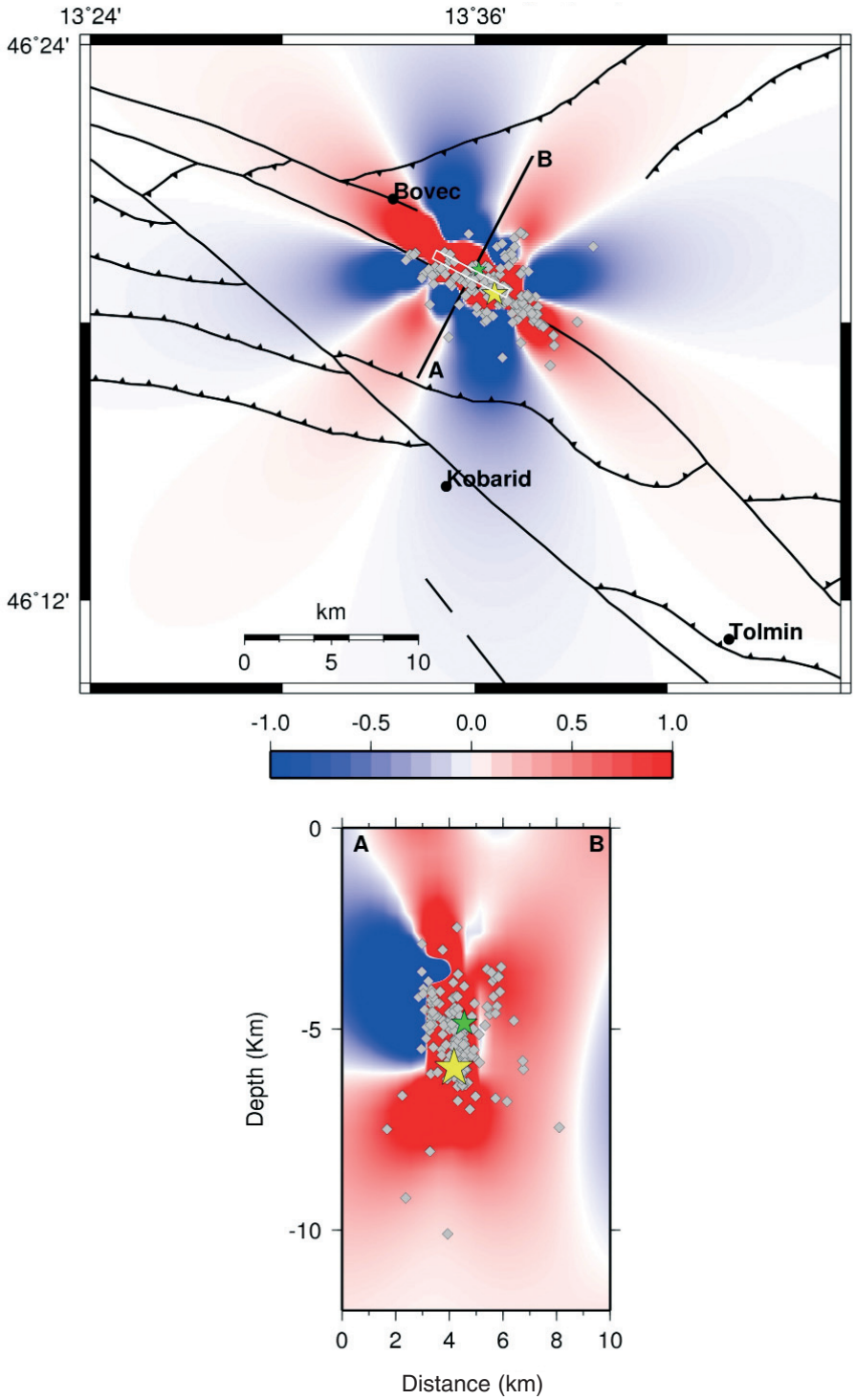

Fig. 13 - Shear stress changes (in bar) caused by the 2004 Kobarid mainshock, taking into account the regional stress field. Map orientations and symbols are as in Figs. 9 and 2.

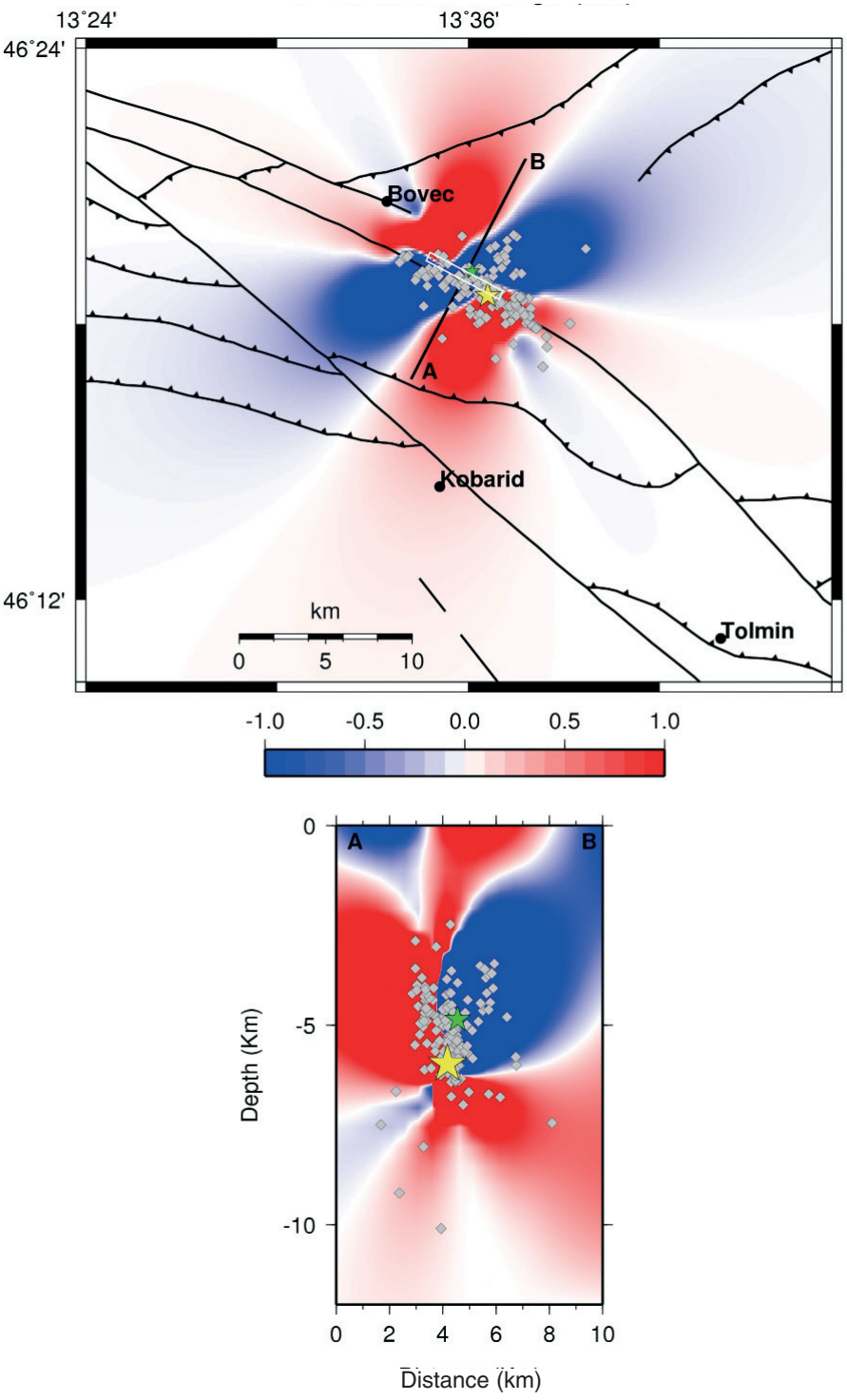

Fig. 14 - Normal stress changes (in bar) caused by the 2004 Kobarid mainshock, taking into account the regional stress field. Map orientations and symbols are as in Figs. 9 and 2.

$$M_{0m} + \sum_{j=1}^{i} M_{0j} = a + b \cdot \ln t_i \tag{5}$$

where

$$a = V_i \, d\sigma, \quad b = V_i \, RT / \gamma, \quad V_i = V_0 + \sum_{j=1}^{i} V_j \tag{6}$$

V_i cumulative focal volume, V_0 focal volume of mainshock, V_j focal volume of the j-th aftershock, M_{0m} seismic moment of the mainshock and M_{0j} seismic moment of the j-th aftershock.

The smallest magnitude chosen for the catalogue completeness is 1.5 for the 2002 Mount Sernio sequence and 2.0 for the 2004 Kobarid sequence. The earthquakes selected for the completeness of the catalogue are 37 for the 2002 sequence (time window 2374 hours) and 167 for the 2004 sequence (time window 3294 hours).

Figs. 15 and 16 show the 2002 and 2004 sequences, respectively, modelled with Eq. (5) using a least square regression and the correlation coefficient r. Seismic moments are obtained from M_D using the following relation (Franceschina *et al.*, 2006):

$$\log M_0 = 8.83 + 1.46 M_D. \tag{7}$$

5. Discussion

The aftershock sequences have been investigated following two different approaches. The static stress changes modelling is based on the Coulomb criterion for shear failure, which considers the strength of the materials. The time behaviour of cumulative seismic moment released during the sequence is derived from a model based on the static fatigue process or delayed brittle fracture. It should be noted that a positive increase in Coulomb stress changes of an earthquake represents a required condition, but not sufficient for triggering another earthquake. This condition means that the fault of the second earthquake is close to the failure state and can be triggered by a positive increase in Coulomb failure function induced by the previous earthquake. The static fatigue model implies that the strength of brittle materials is time dependent. With this model the aftershocks occur on the asperities in and around the mainshock fault that fail after an elapsed time proportional to the stress intensity factor.

The modelling of the Coulomb stress variations of the 2002 Mount Sernio (Figs. 3, 4 and 5) mainshock, calculated on the receiver fault of the largest aftershock, shows that only the positive normal stress changes provide the best correlation with the spatial pattern of many aftershocks. We emphasize that the Coulomb stress variations are calculated with a smooth slip model of the fault, that produces a zone of stress decrease (stress shadow) on the fault plane. According to Lin and Stein (2004), the size of the stress shadow zone related to a thrust earthquake is influenced by the ratio length/width of the fault. As still further pointed out by Lin and Stein (2004), the aftershocks of a thrust fault appear sensitive to normal stress changes. Positive normal stress changes mean a decrease in normal stress, or extension, corresponding to an unclamping effect. The decrease in normal stress can be effective as an increase in shear stress in promoting failure.

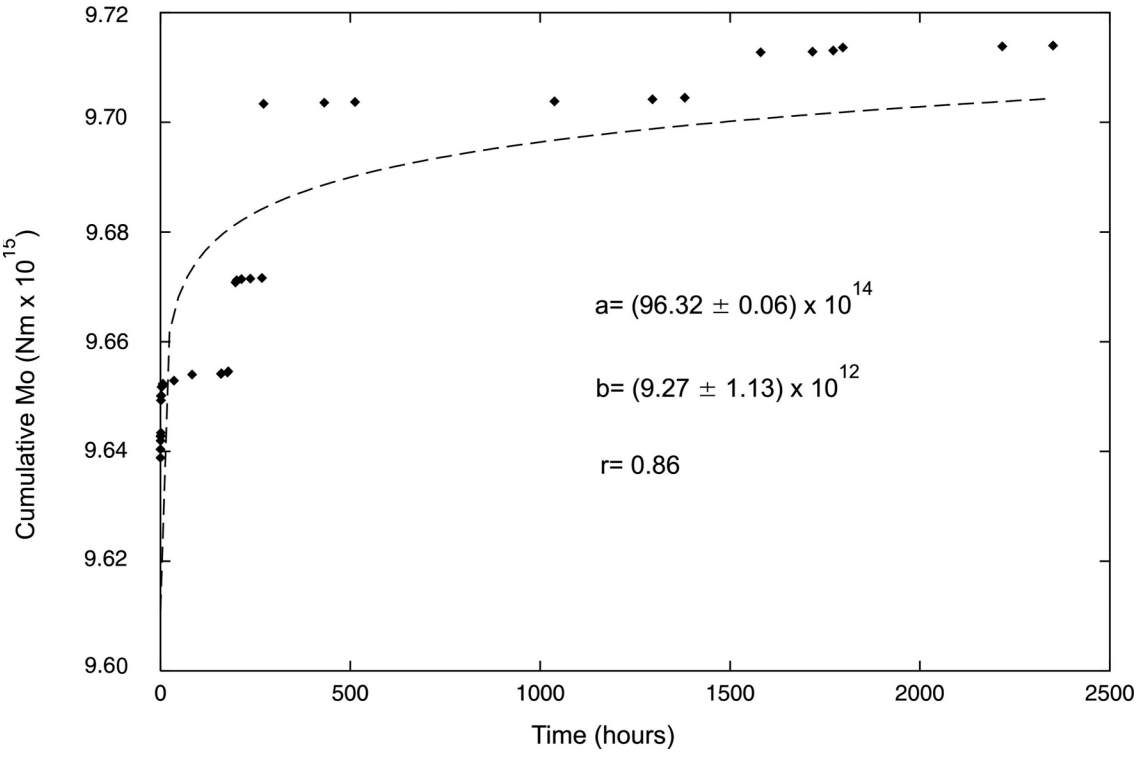

Fig. 15 - Fit (dashed line) of Marcellini's (1995a, 1995b) aftershock model to the 2002 Mount Sernio sequence (diamonds). The cumulative seismic moment is expressed in Nm. The parameters *a* and *b*, with standard deviation, obtained by regressing Eq. (5) and the correlation coefficient *r* are shown.

Laboratory experiments of Linker and Dieterich (1992) demonstrated that relatively small reduction in normal stress causes changes in shear strength and, therefore, in the resistance to sliding. The decrease of normal stress on a fault plane causes a reduction of the fault friction and consequently a reduction in the resistance to sliding.

The modelling of the Coulomb stress variations (Figs. 9, 10 and 11) of the 2004 Kobarid mainshock, calculated on the receiver fault of the largest aftershock, is not sufficient to forecast the spatial pattern of the aftershocks. Most of the earthquakes are located in a stress shadow zone.

The effect of the regional stress field, included in the calculation of Coulomb stress changes, leads to better results for the analyzed sequences. In the case of the 2002 sequence, the patterns of Coulomb stress changes (Fig. 6) and the separate contributions of shear (Fig. 7) and normal (Fig. 8) stress changes are slightly altered, little improving the correlation between the aftershock locations and the areas of positive Coulomb stress variations. About 50 % of the aftershocks are located in the positive Coulomb and shear stress change areas. The positive normal stress changes provide again the best correlation with the largest percentage of earthquakes (65%).

The pattern of the Coulomb variations of the 2004 Kobarid mainshock changes significantly when the effect of the regional stress field is considered and a positive correlation is found between the Coulomb (Fig. 12) and the shear (Fig. 13) stress variations and the location of most aftershocks (about 75%). The positive normal stress changes region (Fig. 14) are again associated

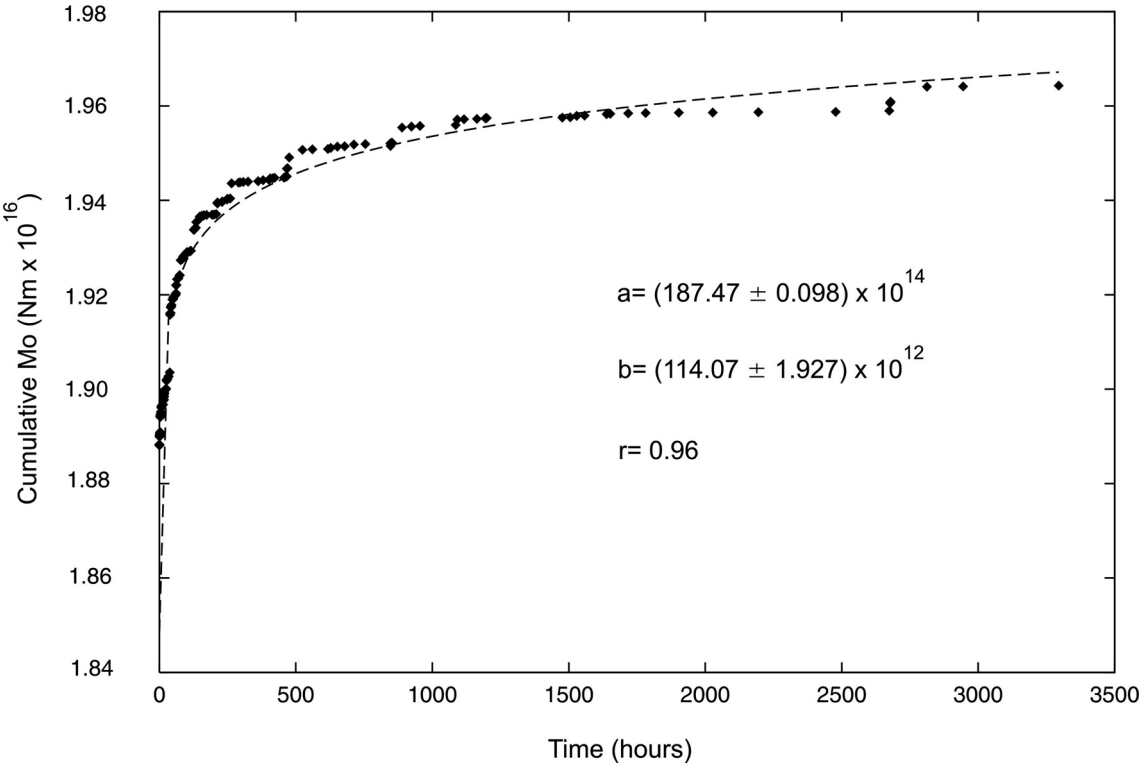

Fig. 16 - Fit (dashed line) of Marcellini's (1995a, 1995b) aftershock model to the 2004 Kobarid sequence (diamonds). The cumulative seismic moment is expressed in Nm. The parameters *a* and *b*, with standard deviation, obtained by regressing Eq. (5) and the correlation coefficient *r* are shown.

to a minor percentage of earthquakes (about 38%).

We remind that the model (King *et al.*, 1994) is more sensitive to the orientation of regional stress than the regional stress amplitude and the coefficient of effective friction. The modelling that incorporates the regional stress field produced Coulomb and shear stress changes that well correlate with the spatial aftershock distribution of the 2004 Kobarid sequence. The contribution of the regional stress field has slightly changed the pattern of the Coulomb stress variations of the Mount Sernio 2002 sequence. The off-fault aftershocks appear mainly located in the Coulomb stress increase areas. The smooth slip modelling of the rupture plane predicts in any case a stress shadow on the thrust main fault where some aftershocks are located. As emphasized by Cocco *et al.* (2000), this represents a lack of the model in predicting Coulomb stress interaction for events close in space and time. This aspect can be explained by different factors.

The nucleation of aftershocks close to the rupture plane is probably conditioned by stress heterogeneities on the fault plane caused by small-scale discontinuities not represented by smooth slip models of the Coulomb failure function (Lin and Stein, 2004).

Helmstetter and Shaw (2006) showed that Coulomb stress change heterogeneity modifies the temporal evolution of the seismicity rate, compared to a uniform stress change. Hu *et al.* (2009) demonstrated that crustal heterogeneities can significantly affect the static stress changes after a

mainshock and, therefore, the earthquake triggering.

Smith and Dieterich (2010) presented a model of aftershock sequences that integrates 3D Coulomb static stress changes, rate-state seismicity equations, slip on geometrically complex faults and spatially heterogeneous fault plane/slip directions. The simulation resulted appropriate to explain the activation of aftershocks in traditional stress shadow regions predicted by the Coulomb static stress change analysis. In this model, the aftershock triggering is mostly controlled by the spatially heterogeneous initial crustal stress and the slip on geometrically complex faults.

Finally, we emphasize that the aftershock pattern can be strongly influenced by the coupling of fluid flow and elastic deformation. The mainshock alters the state of stress in the volume surrounding the fault zone, causing a time-dependent adjustment of local pore pressure and consequent time dependent effects on the stress variations. Miller *et al.* (2004) proposed that the aftershocks of the 1997 Umbria-Marche (Italy) sequence may be driven by a high-pressure pulse generated from the coseismic release of trapped high-pressure carbon dioxide. The high pressure pulse propagated into the damaged zone generated by the mainshock and triggered the aftershocks by lowering the effective normal stress. Bosl and Nur (2002) claimed that the temporal pattern of the aftershocks is related to the time dependent process of fluid flow. After an earthquake, pore fluids flow from regions of high pressure to regions of low pressure. The permeability of the rocks influences the rate of relaxation and the flow paths. The role played by pore fluid diffusion in the pattern of Coulomb stress changes generated by a mainshock can be complex. Piombo *et al.* (2005) demonstrated that the Coulomb stress changes caused by a shear dislocation may be initially negative in some zones, but become positive as pore fluids are redistributed and there are also regions where the Coulomb stress changes vary from positive to negative. They concluded that all these aspects cannot be evaluated by the static stress changes analysis.

Different features characterize the temporal behaviour of cumulative seismic moment released in the 2002 and 2004 aftershock sequences. The least-squares regression analysis exhibits different value of r. The 2002 sequence is characterized by evident steps in the cumulative seismic moment release (Fig. 15). The released seismic moment with time of the 2004 sequence (Fig. 16) is quite well modelled by Eq. (5), even if some minor steps in the cumulative seismic moment are recognizable. Figs. 15 and 16 evidence that many aftershocks occur in the hours immediately following the mainshock. The asperities located in the neighbourhood of the mainshock fault undergo to large stress close to the stress state of the mainshock and, therefore, break in a short time. We recall that the stress at the origin time of the mainshock is given by the sum of static stress (fracture stress) just before the event and the stress contribution induced by the dynamic rupture of the mainshock (Marcellini, 1995a). The relation between the cumulative seismic moment and the elapsing time after the mainshock is based on the uniformity statement of the mainshock stress change. More is the ratio between static stress and dynamic stress step, the more uniform is the mainshock stress change (Marcellini, 1997). Therefore, the quality of the fit is an indicator of the distribution of stress in the volume surrounding the mainshock. The better the fit is, the more the distribution of stress on the asperities is uniform. Departures from the fit suggest stress concentrations or not uniform conditions of stress as expected by the static fatigue model. Such behaviour was explained by Scholz (1972) in static fatigue experiments

because of fluctuations in the strength of rocks. According to Scholz (1968), the brittle fracture of rock is a cumulative process involving a complex evolution of small scale fracturing which leads to overall fracture. This behaviour is caused by the mechanical heterogeneities of the medium which produces fluctuations in the stress field. Sharp variations in the mechanical properties can produce sharp changes in the aftershock time sequence. Following these considerations, the 2002 sequence is affected by higher stress heterogeneity.

We remind that the spatial variations of the stress induced by the mainshock are not considered in the static fatigue model (Marcellini, 1997).

6. Conclusions

The aftershock sequences triggered by the 2002 M_D 4.9 and the 2004 M_D 5.1 mainshocks have been analyzed with the methods based on Coulomb stress changes modelling and on a static fatigue approach. The Coulomb stress changes, calculated on the receiver fault of the largest aftershock, show that most of the aftershock sequences is located in a stress shadow zone. The normal stress changes of the 2002 sequence provide the best correlation with the aftershock pattern, attributable to a mechanism of unclamping. The contribution of the regional stress in the 2002 sequence slightly improves the correlation between the positive Coulomb and shear stress change areas and the aftershock pattern. The regional stress field modifies significantly the pattern of the Coulomb stress variation induced by the 2004 mainshock, providing a good correlation between the positive Coulomb and the shear stress changes, and the location of the aftershocks. Generally, the models that incorporate the regional stress field fit better the spatial patterns of the aftershocks. Therefore, the patterns of the Coulomb stress field and of the aftershocks appear to be controlled by the orientation of the regional stress. However, the results obtained show that solely accounting for regional stress is not sufficient to fit completely the aftershock pattern.

This aspect can be attributed to some factors not accounted in the model of Coulomb static stress interactions:

- heterogeneity of the stress changes;
- mechanical heterogeneity in the crustal volume considered;
- time dependent effects caused by pore pressure relaxation.

Stress fluctuations induced by the mechanical heterogeneities of medium is suggested by the static fatigue modelling, particularly for the 2002 sequence. The cumulative seismic moment release versus time evidences different behaviour between the 2002 and the 2004 sequences. The 2004 sequence appears better modelled than the 2002 sequence. The results evidence that the distribution of stress of the 2004 sequence is more uniform than the 2002 sequence. The model is based on the uniformity statement of the mainshock stress change. The static fatigue model implies that the fit of the log-linear relation of seismic moment release with time is related to the distribution of stress in the volume surrounding the mainshock fault. Departures from the fit are related to stress concentrations, caused in the static fatigue process by the mechanical heterogeneities of the medium. According to this model, the 2002 sequence is affected by stress heterogeneity.

Acknowledgements The static stress changes have been calculated with the Coulomb 3.2 software package of S. Toda, R. Stein, J. Lin and V. Sevilgen. We are indebted with S. Gentili for her helping in graphics of the pattern of Coulomb failure function. We thank F. Gentile for the relocation of the seismic sequences and S. Urban for his assistance. The seismometric network of Friuli Venezia Giulia is managed by OGS with financial support by the Civil Protection of the Friuli Venezia Giulia Region.

REFERENCES

Bosl W.J. and Nur A.; 2002: *Aftershocks and pore fluid diffusion following the 1992 Landers earthquake.* J. Geophys. Res., **107**, B12, doi:10.1029/2001JB000155.

Bressan G., Bragato P.L. and Venturini C.; 2003: *Stress and strain tensors based on focal mechanisms in the seismotectonic framework of the Eastern Southern Alps.* Bull. Seismol. Soc. Am., **93**, 1280-1297.

Bressan G., Gentile G.F., Perniola B. and Urban S.; 2009: *The 1998 and 2004 Bovec-Krn (Slovenia) seismic sequences: aftershock pattern, focal mechanisms and static stress changes.* Geophys. J. Int., **179**, 231-253.

Cocco M., Nostro C. and Ekström G.; 2000: *Static stress changes and fault interaction during the 1997 Umbria-Marche earthquake sequence.* J. Seismolog., **4**, 501-516.

Dieterich J.H.; 1994: *A constitutive law for rate of earthquake production and its application to earthquake clustering.* J. Geophys. Res., **99**, 2601-2618.

Franceschina G., Kravanja S. and Bressan G.; 2006: *Source parameters and scalino relationships in the Friuli-Venezia Giulia (Northeastern Italy) region.* Phys. Earth Planet. Int., **154**, 148-167.

Gentile G.F., Bressan G., Burlini L. and de Franco R.; 2000: *Three-dimensional Vp and Vp/Vs models of the upper crust in the Friuli area (Northeastern Italy).* Geophys. J. Int., **141**, 457-478.

Gentili S. and Bressan G.; 2008: *The partitioning of radiated energy and the largest aftershock of seismic sequences occurred in the northeastern Italy and western Slovenia.* J. Seismolog., **12**, 343-354.

Harris R.A.; 1998: *Introduction to special section: stress triggers, stress shadows, and implications for seismic hazard.* J. Geophys. Res., **103,** 24347-24358.

Helmstetter A. and Shaw B.E.; 2006: *Relation between stress heterogeneity and aftershock rate in the rate-and-state model.* J. Geophys. Res., **111**, B07304, doi:10.1029/2005JB004077.

Hu C., Zhou Y., Cai Y. and Wang C.; 2009: *Study of earthquake triggering in a heterogeneous crust using a new finite element model.* Seismol. Res. Lett., **80**, 799-807.

Kastelic V., Vrabec M., Cunningham D. and Gosar A.; 2008: *Neo-Alpine structural evolution and present-day tectonic activity of the eastern Southern Alps: the case of the Ravne Fault, NW Slovenia.* J. Struct. Geol., **30**, 963-975.

King G.C.P., Stein R.S. and Lin J.; 1994: *Static stress changes and the triggering of earthquakes.* Bull. Seismol. Soc. Am., **84**, 935-953.

Lin J. and Stein R.S.; 2004: *Stress triggering in thrust and subduction earthquakes and stress interaction between the southern San Andreas and nearby thrust and strike-slip faults.* J. Geophys. Res., **109**, B02303, doi:10.1029/2003JB002607.

Linker M.F. and Dieterich J.H.; 1992: *Effects of variable normalstress on rock friction: observations and constitutive equations.* J. Geophys. Res., **97,** 4923-4940.

Madariaga R.; 1979: *On the relation between seismic moment and stress drop in the presence of stress and strength heterogeneity.* J. Geophys. Res., **84**, 2243-2250.

Marcellini A.; 1995a: *Arrhenius behavior of aftershock sequences.* J. Geophys. Res., **100**, 6463-6468.

Marcellini A.; 1995b: *Correction to 'Arrhenius behavior of aftershock sequences.* J. Geophys. Res., **100**, 20409.

Marcellini A.; 1997: *Physical model of aftershock temporal behaviour*. Tectonophys., **277**, 137-146.

Miller A.S, Collettini C., Chiaraluce L., Cocco M., Barchi M. and Kaus B.J.P.; 2004: *Aftershock driven by a high-pressure CO_2 source at depth.* Nature, **27**, 724-727.

Nostro C., Cocco M. and Belardinelli M.E.; 1997: *Static stress changes in extensional regimes: an application to*

southern Apennines (Italy). Bull. Seismol. Soc. Am., **87**, 234-248.

Okada Y.; 1992: *Internal deformation due to shear and tensile faults in a half-space.* Bull. Seismol. Soc. Am., **82**, 1018-1040.

Perniola B., Bressan G. and Pondrelli S.; 2004: *Changes in failure stress and stress transfer during the 1976-77 Friuli earthquake sequence.* Geophys. J. Int., **156**, 297-306.

Piombo A., Martinelli G. and Dragoni M.; 2005: *Post-seismic fluid flow and Coulomb stress changes in a poroelastic medium.* Geophys. J. Int., **162**, 507-515.

Rebez A. and Renner G.; 1991: *Duration magnitude for the northeastern Italy seismometric network.* Boll. Geof. Teor. Appl., **33**, 177-186.

Rice J.R.; 1992: *Fault stress states, pore pressure distributions and the weakness of the San Andreas fault.* In: Evans B. and Wong T.F. (eds), Fault mechanics and transport properties of rock, Academic Press, San Diego, CA, USA, pp. 475-503.

Roeloffs L.A.; 1988: *Fault stability changes induced beneath a reservoir with cyclic variations in water level.* J. Geophys. Res., **93,** 2107-2124.

Saraò A.; 2006: *Seismic moment determination at CRS.* Annual Report CRS-INOGS.

Scholz C.H.; 1968: *Microfractures, aftershocks and seismicity*. Bull. Seismol. Soc. Am., **58**, 1117-1130.

Scholz C.H.; 1972: *Static fatigue of quartz*. J. Geophys. Res., **77**, 2104-2114.

Scholz C.H.; 1990: *The mechanics of earthquakes and faulting.* Cambrige University Press, UK, 439 pp.

Smith D.E. and Dieterich J.H.; 2010: *Aftershock sequences modeled with 3-D stress heterogeneity and rate-state seismicity equations: implications for crustal stress estimation.* Pure Appl. Geophys., **167**, 1067-1085.

Stein R.S., King G.C.P. and Lin J.; 1994: *Stress triggering of the 1994 M=6.7 Northridge, California, earthquake by its predecessors.* Science, **265**, 1432-1435.

Toda S., Stein R.S., Richards-Dinger K. and Bozkurt S.B.; 2005: *Forecasting the evolution of seismicity in southern California: animations built on earthquake stress transfer.* J. Geophys. Res., **110**, B05S16, doi:10.1029/2004JB003415.

Wells D.L. and Coppersmith K.J.; 1994: *New empirical relationships among magnitude, rupture length, rupture width, rupture area and surface displacement*. Bull. Seismol. Soc. Am., **84**, 974-1002.

Zhurkov S.N.; 1965: *Kinetic concept of the strength of solids.* Int. J. Fract. Mech., **1**, 311-323.

Corresponding author: Gianni Bressan
Istituto Nazionale di Oceanografia e di Geofisica Sperimentale, Dip. C.R.S.
via Treviso, 55 , C.P. 1, Cussignacco (Udine), Italy
Phone: +39 0432 522433; fax: +39 0432 522474; e-mail: gbressan@inogs.it